Heat shock protein 90–mediated inactivation of nuclear factor-κB switches autophagy to apoptosis through *becn1* transcriptional inhibition in selenite-induced NB4 cells

Qian Jiang, Yuhan Wang, Tianjiao Li, Kejian Shi, Zhushi Li, Yushi Ma, Feng Li, Hui Luo, Yang Yang, and Caimin Xu

National Laboratory of Medical Molecular Biology; Institute of Basic Medicine Sciences and School of Basic Medicine, Peking Union Medical College and Chinese Academy of Medical Sciences, Beijing 100005, China

ABSTRACT **Autophagy can protect cells while also contributing to cell damage, but the precise interplay between apoptosis and autophagy and the contribution of autophagy to cell death are still not clear. Previous studies have shown that supranutritional doses of sodium selenite promote apoptosis in human leukemia NB4 cells. Here, we report that selenite treatment triggers opposite patterns of autophagy in the NB4, HL60, and Jurkat leukemia cell lines during apoptosis and provide evidence that the suppressive effect of selenite on autophagy in NB4 cells is due to the decreased expression of the chaperone protein Hsp90 (heat shock protein 90), suggesting a novel regulatory function of Hsp90 in apoptosis and autophagy. Excessive or insufficient expression indicates that Hsp90 protects NB4 cells from selenite-induced apoptosis, and selenite-induced decreases in the expression of Hsp90, especially in NB4 cells, inhibit the activities of the IκB kinase/nuclear factor-κB (IKK/NF-κB) signaling pathway, leading to less nuclear translocation and inactivation of NF-κB and the subsequent weak binding of the *becn1* promoter, which facilitates the transition from autophagy to apoptosis. Taken together, our observations provide novel insights into the mechanisms underlying the balance between apoptosis and autophagy, and we also identified Hsp90–NF-κB–Beclin1 as a potential biological pathway for signaling the switch from autophagy to apoptosis in selenite-treated NB4 cells.**

Monitoring Editor
Kunxin Luo
University of California, Berkeley

Received: Oct 29, 2010
Revised: Jan 28, 2011
Accepted: Feb 14, 2011

INTRODUCTION

Autophagy and apoptosis are two distinct, tightly regulated biological processes that both play critical roles in development, pathology, and disease (Tsujimoto and Shimizu, 2005; Maiuri *et al.*, 2007). Autophagy is characterized by the sequestration of cytoplasmic materials into autophagosomes for bulk degradation by lysosomes, and its function in tumorigenesis remains highly controversial. Some studies have demonstrated that autophagy contributes to cell survival by adapting cells to stress conditions, whereas others also describe autophagy as "type-II" cell death because cell death is preceded or accompanied by massive autophagic vacuolization in some situations (Daniel and Scott, 2000; Levine and Yuan, 2005; Karantza-Wadsworth and White, 2007). Apoptosis, the "type-I" programmed cell death, is an innate suicide program highly controlled by multiple signals. Increasing evidence points to a complex interplay between autophagy and apoptosis (Portugal *et al.*, 2009), but the precise mechanism regulating this phenomenon remains unknown.

Selenium is an essential trace element with chemopreventive potential against various cancers (Sinha and El-Bayoumy, 2004; Asfour *et al.*, 2006; Sanmartin *et al.*, 2008). Our previous work has shown

This article was published online ahead of print in MBoC in Press (http://www.molbiolcell.org/cgi/doi/10.1091/mbc.E10-10-0860) on February 23, 2011.

Address correspondence to: Caimin Xu (caiminxu@yahoo.com.cn).

Abbreviations used: 17-AAG, 17-allylamino-demethoxygeldamycin; 3-MA, 3-methyladenine; CAPE, caffeic acid phenethyl ester; ChIP, chromatin immunoprecipitation; DAPI, 4′,6-diamidino-2-phenylindole; ER, endoplasmic reticulum; FACS, fluorescence-activated cell sorting; FITC, fluorescein isothiocyanate; Hsp90, heat shock protein 90; IKK, IκB kinase; LC3, microtubule-associated protein-1 light chain-3; MDC, monodansylcadaverine; mTOR, mammalian target of rapamycin; NF-κB, nuclear factor-κB; PARP, poly (ADP-ribose) polymerase; PBS, phosphate-buffered saline; pCMV, plasmid cytomegalovirus; PI3KC3, phosphatidylinositol-3-kinase class III; RT, reverse transcription; UVRAG, UV irradiation resistance-associated gene.

that sodium selenite at 20 μmol/l promotes mitochondrial damage and endoplasmic reticulum (ER) stress in human acute promyelocytic leukemia–derived NB4 cells with decreased autophagic levels and that the direct inhibition of autophagy enhances selenite-induced apoptosis (Li *et al.*, 2003; Guan *et al.*, 2009; Ren *et al.*, 2009). Unexpectedly, however, similar treatments administered to two leukemia cell lines, HL60 and Jurkat, resulted in different patterns of cell death, which prompted us to explore the specific signaling pathway that regulated the switch from autophagy to apoptosis in NB4 cells. Pathway-focused microarrays combine microarray data and pathway information; thus they may highlight the processes taking place in cells and tissues and provide insights into the tissue- and process-specific functioning of the genome. Pathway-focused microarrays greatly shorten the time needed to find potential biomarkers for disease treatment, and they have become effective tools to study biological pathways. Therefore reverse transcription (RT)-PCR autophagy array technology was first performed to screen for important regulators from 84 key genes, including autophagy machinery components and regulators. Next heat shock protein 90 (Hsp90) was identified as a potential key regulator, and its importance in autophagy/apoptosis was subsequently confirmed. Hsp90 is an abundant cytosolic chaperone (1–2% of cytosolic protein) required for the stability and function of numerous client proteins that play critical roles in signal transduction, cellular trafficking, chromatin remodeling, cell growth, differentiation, and reproduction (Neckers and Ivy, 2003; Cullinan and Whitesell, 2006; Mahalingam *et al.*, 2009). In most cancer cells, the hyperactivation of Hsp90 stabilizes its client proteins and protects cells from stress conditions (Zuehlke and Johnson, 2010). In contrast, the specific inhibition of Hsp90 by some chemicals can lead to degradation of its clients via either the ubiquitin proteasome system or autophagy (Qing *et al.*, 2007).

There are some inherent relationships between autophagy and Hsp90 (Qing *et al.*, 2006). Recent studies have reported that IκB kinase (IKK), an essential activator of NF-κB, is a client protein of Hsp90 that can be selectively degraded by autophagy when Hsp90 is inhibited. Consequently the inhibited nuclear translocation of NF-κB leads to various changes in cellular programs (Qing *et al.*, 2006, 2007; Xiao, 2007). Beclin1, the first mammalian autophagy protein to be described, appears to act as a nexus between autophagy and apoptosis (Pattingre *et al.*, 2005), and recent studies have suggested that there are three NF-κB binding sites (κB sites) inside the first intron of the *becn1* promoter (Copetti *et al.*, 2009a, 2009b). Therefore the aim of this study was to determine whether Hsp90 causes irreversible apoptotic cell death by negatively regulating autophagy in selenite-treated NB4 cells and to assess how the IKK/NF-κB pathway functions in directing the cell toward an ultimate fate of either autophagy or apoptosis.

RESULTS

Sodium selenite specifically suppressed autophagy during apoptosis in NB4 cells

The cleaved form of poly (ADP-ribose) polymerase (PARP) and caspase3 were detected after NB4, HL60, and Jurkat cells were exposed to 20 μM sodium selenite for 24 h (Figure 1, A–C), indicating that apoptosis was apparently induced by selenite in all three human leukemia cell lines. Consequently p62, Beclin1, and the conversion of microtubule-associated protein-1 light chain-3 (LC3)I/II were used as markers to determine the effect of selenite on autophagy. Following exposure to selenite, both HL60 and Jurkat cells exhibited p62 degradation, LC3I to LC3II conversion, and Beclin1 up-regulation (Figure 1, B and C), suggesting the concurrence of autophagy and apoptosis. In NB4 cells, however, autophagy was suppressed gradually during apoptosis after selenite treatment (Figure 1A). Vesicular accumulation of LC3 is a marker of autophagy, and the immunofluorescence staining showed punctate staining of LC3-positive autophagic vesicles in untreated but not in selenite-treated NB4 cells (Figure 1D). The treatment of NB4 cells with 3-methyladenine (3-MA), a well-known inhibitor of the initial stage of conventional autophagy, also decreased the punctate distribution of LC3 compared with what was observed in untreated cells (Figure 1D). Nevertheless, selenite treatment in HL60 and Jurkat cells altered the pattern of LC3 staining in the cytosol from a diffuse pattern to a punctate pattern (Figure 1D), which was characteristic of increased levels of autophagosomes. Additionally, we stained cells with the autofluorescent base monodansylcadaverine (MDC; Iwai-Kanai *et al.*, 2008; Biederbick *et al.*, 1995) to detect the autophagic vacuoles. Fluorescence microscopy revealed that selenite inhibited the appearance of MDC-positive granular structures in NB4 cells, whereas the punctate distribution of MDC fluorescence was enhanced in HL60 and Jurkat cells (Figure 1E). The quantification of MDC-positive cells is shown in Figure 1F, which further confirms our previous results. Collectively, these data demonstrated significantly different effects of selenite on autophagy between NB4 and the other two cell lines.

Autophagy antagonized selenite-induced NB4 apoptosis and the inhibition of autophagy-sensitized cells to apoptosis

The cross-talk between apoptosis and autophagy is complex and sometimes contradictory. It varies among cell and stress types. To determine the effect of autophagy on apoptosis in selenite-treated NB4 cells, we assayed autophagy marker proteins in the presence of selenite plus 3-MA or bafilomycin A1, which inhibits autophagosome formation or blocks downstream autophagosome–lysosome fusion, respectively. The amounts of cleaved PARP and caspase3 production were greatly increased in the combined treatment group (Figure 2A, lines 1 and 2). The inhibitory efficiency was confirmed in Figure 2A (lines 3, 4, and 5). Additionally, fluorescence-activated cell sorting (FACS) analysis indicated the presence of significantly increased cell apoptotic rates when autophagy was inhibited (Figure 2B). These results suggest that autophagy inhibition sensitizes NB4 cells to selenite-induced apoptosis.

To further test whether selenite-induced NB4 apoptosis is dependent on autophagy inhibition, the potent autophagy activators, rapamycin and GF109203X (Jiang *et al.*, 2010), which inhibit the activity of mammalian target of rapamycin (mTOR) and PKC, respectively, were added to cells for 1.5 h before selenite treatment (Figure 2C, lines 3, 4, and 5). Western blot and FACS analysis showed that excessive autophagosome formation attenuated selenite-caused cell apoptosis (Figure 2, C and D). The analysis suggested that autophagy acted as an antagonist to block apoptotic cell death by promoting cell survival in selenite-treated NB4 cells.

Bioinformatic analyses of an autophagy RT-PCR array and the identification of Hsp90 in selenite-suppressed autophagy

We have shown that selenite can facilitate cell signal switching from autophagic protection to irreversible apoptotic death in NB4 cells; therefore microarray analysis was performed with the Human Autophagy RT^2 Profiler PCR Array (SABiosciences, Frederick, MD) to screen for the potential regulators in switching apoptotic and autophagic processes. As shown in Figure 3A, selenite treatment reduced the expression of most autophagy-related genes in a time-dependent manner: *ATG1, ATG3, ATG5, ATG6/BECN1, ATG7, ATG9A, ATG9B, ATG12, ATG16L1, ATG16L2,* and so forth.

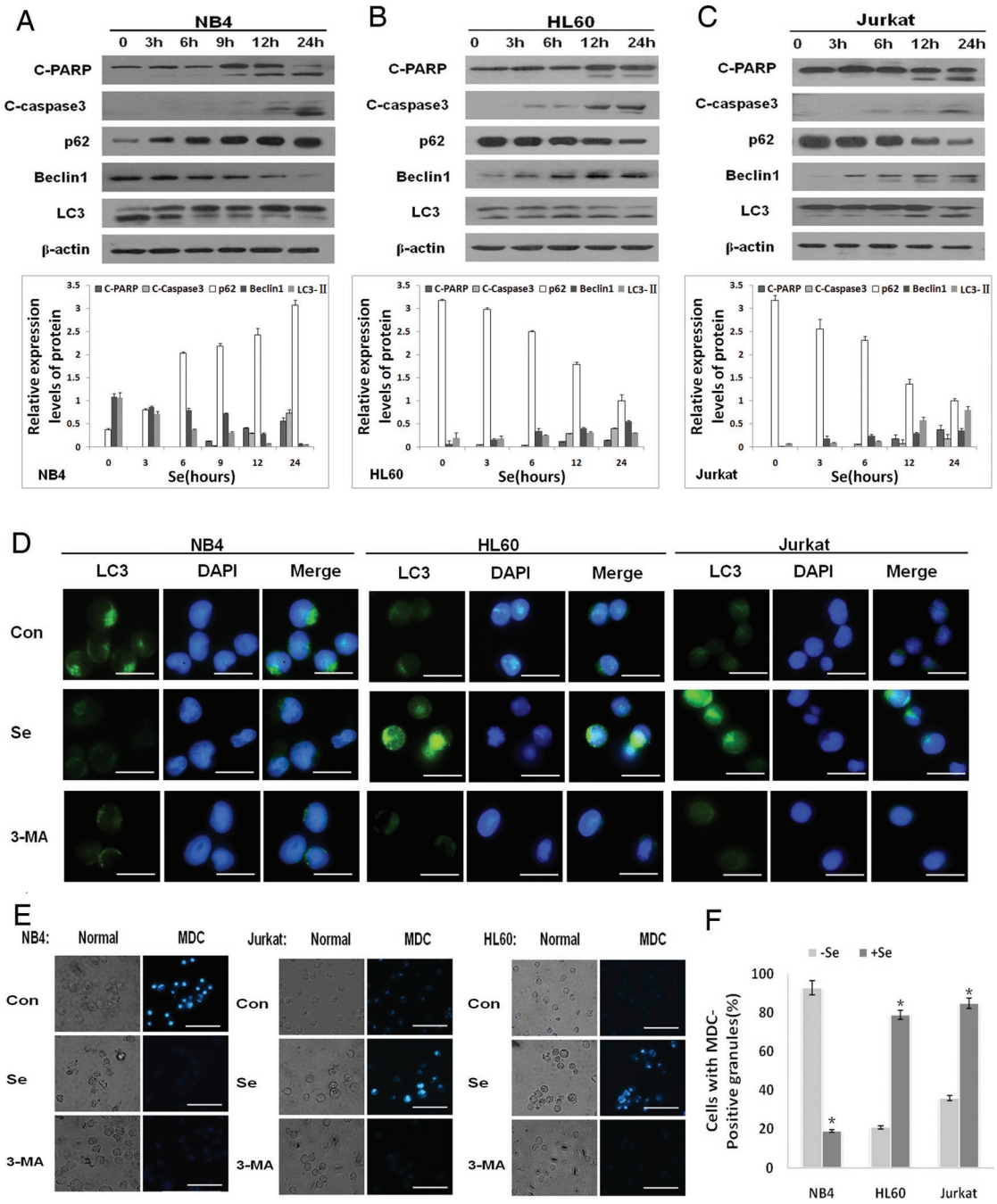

FIGURE 1: Sodium selenite specifically suppressed autophagy during apoptosis in NB4 cells. (A–C) The effect of sodium selenite on apoptosis- and autophagy-related genes in human leukemia cells. NB4, HL60, and Jurkat cells were treated with sodium selenite (20 μmol/L) for different times as indicated. Then, cleaved-PARP, cleaved-caspase3, p62, Beclin1, and LC3 were detected by Western blot. The top panels show representative Western blots, and the bottom panels show the quantification of protein levels normalized to those of the β-actin control. (D) Immunofluorescence staining of LC3 in human leukemia cells. Cells were treated with selenite (20 μmol/l) or 3-MA (1 mmol/l) for 24 h. After fixation, the cells were immunostained with anti-LC3 antibody (green). The nuclei were stained by DAPI (blue). The scale bar represents 20 μm. (E) MDC staining for visualization of autophagic vacuoles in human leukemia cells. NB4, HL60, and Jurkat cells were stained with MDC as described in *Material and Methods*, and staining was detected by fluorescence microscopy. The scale bar represents 100 μm. (F) The percentage of cells with punctate MDC fluorescence was calculated relative to a minimum of 100 cells per sample. Data are presented as the mean ± SD (n = 3). *p < 0.05 compared with control group.

Moreover, the expression of most apoptosis-promoted genes, such as *BAD*, *BAX*, and *P53*, was up-regulated, and the expression of the anti-apoptotic genes *BCL2* and *BCLXL* was down-regulated, as we expected (Figure 3A). Additionally, two kinds of protein chaperones that regulate molecular chaperone-mediated autophagy, Hsp70 and Hsp90, both exhibited a decline after an initial transitory increase (Figure 3B). Because a previous study had indicated that a homologue of Hsp70, Grp78/Bip, had no role in selenite-induced

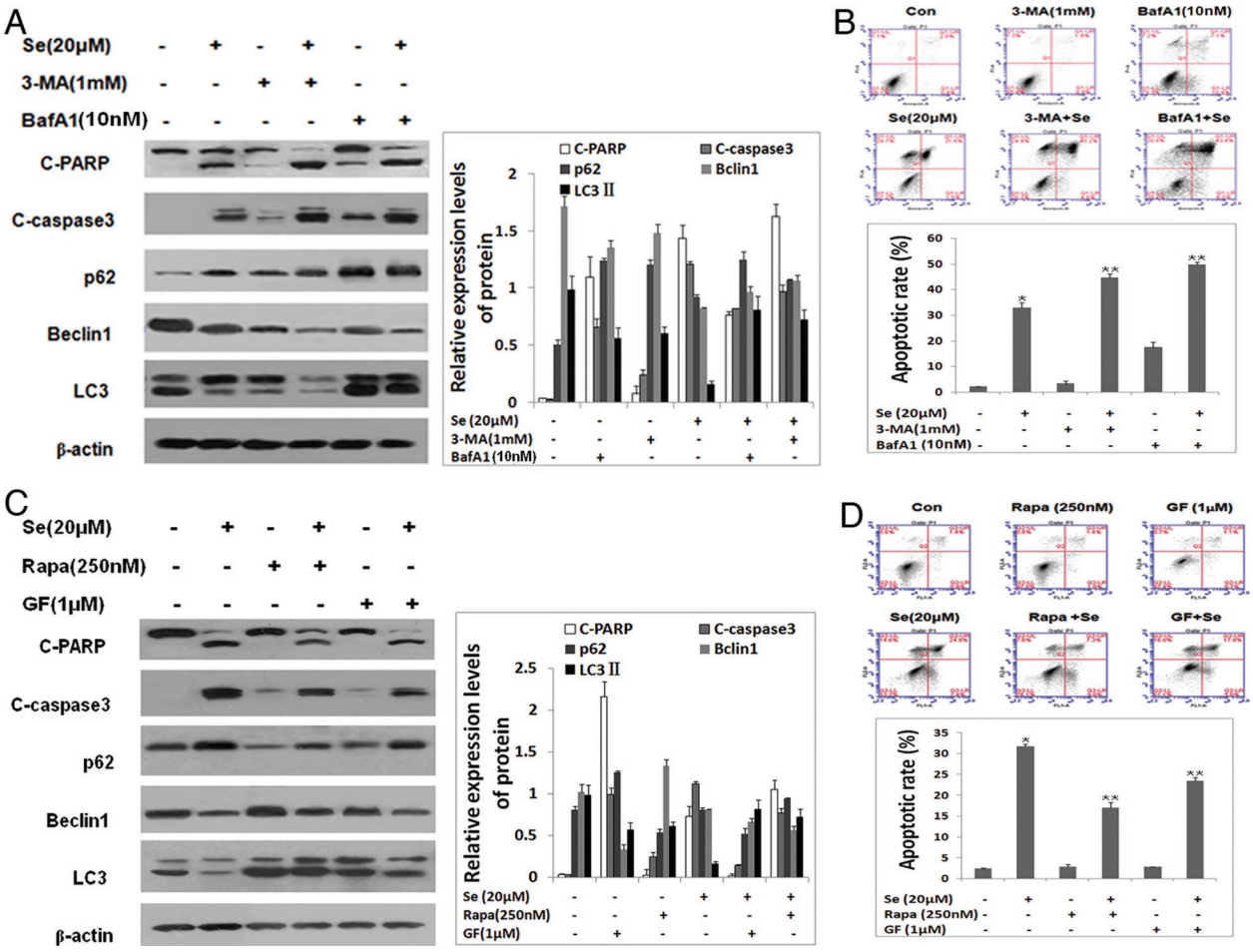

FIGURE 2: Autophagy antagonized selenite-induced NB4 apoptosis, and inhibition of autophagy sensitized cells to apoptosis. (A and C) An autophagy inhibitor, either 3-MA (1 mmol/l) or bafilomycin A1 (10 nmol/l) (A), or an autophagy activator, either Rapamycin (250 nmol/l) or GF109203X (1 μmol/l) (C), was added into NB4 cells for 1.5 h before selenite treatment. Then, cleaved-PARP, cleaved-caspase3, p62, Beclin1, and LC3 were detected by Western blot. The left panels show representative Western blots, and the right panels show the quantification of protein levels normalized to those of the β-actin control. (B and D) The effect of autophagy inhibitors (B) or activators (D) on selenite-induced NB4 apoptosis was analyzed on a flow cytometer using Annexin V/PI staining methods. Data are presented as the mean ± SD (n = 3). *$p < 0.01$ compared with control group. **$p < 0.05$ compared with selenite treatment group.

NB4 apoptosis (Guan *et al.*, 2009), Hsp90 was chosen for further study. Fold changes in Hsp90 transcriptional and translational expression levels in selenite-treated NB4 cells were verified by RT-PCR and Western blot, respectively (Figure 3C). The protein levels of Hsp90 in HL60 and Jurkat cells remained constant, however, after selenite treatment (Figure 3D).

To identify possible reasons for this discrepancy, we checked the p53 status of these cell lines because the tumor suppressor p53 has been shown to function in the transcriptional repression of the *hsp90* gene (Zhang *et al.*, 2004; Habib, 2009). The results showed that our NB4 cell line expressed wild-type p53 and that nuclear p53 expression was increased after selenite exposure. The HL60 and Jurkat lines used here, however, were p53-null cell types (Li *et al.*, 2010; Supplementary Figure S1A). A negative regulatory effect of p53 on Hsp90 expression was observed by inhibiting p53 activity and chromatin immunoprecipitation (ChIP) analysis (Supplementary Figure S1, B and C).

Hsp90 is required for selenite-induced apoptosis

To further evaluate the biological effect of Hsp90 inhibition on apoptosis and autophagy, NB4 cells were transfected via electroporation with the eukaryotic expression vector plasmid cytomegalovirus (pCMV)-Hsp90 to overexpress Hsp90. Successful transfection was confirmed by Western blot analysis (Figure 4A). Selenite-caused cleavage of PARP and caspase3 was nearly completely inhibited when cells were transfected with pCMV-Hsp90 (Figure 4A). The FACS results also revealed that overexpression of Hsp90 protected cells from apoptosis compared with the vacant vector group (negative control) and the nontransfection group (Figure 4B). Moreover, cells overexpressing Hsp90 showed a decrease in p62 and an increase in LC3 II compared with cells treated with selenite alone (Figure 4A), suggesting that increased Hsp90 levels facilitated autophagosome formation.

On the basis of the results just given, we speculated that Hsp90 was required for selenite-regulated apoptosis and autophagy. To confirm this speculation, siRNA was used to reduce endogenous Hsp90 expression in NB4 cells, which resulted in a 60% reduction of Hsp90 protein levels (Figure 4C). As we expected, siRNA knockdown was sufficient to cause cell apoptosis, and a faster apoptotic rate was detected in combination with selenite treatment (Figure 4D). Additionally, Figure 4C shows that knockdown of Hsp90 not only aggravated cleavage of PARP and caspase3 during selenite

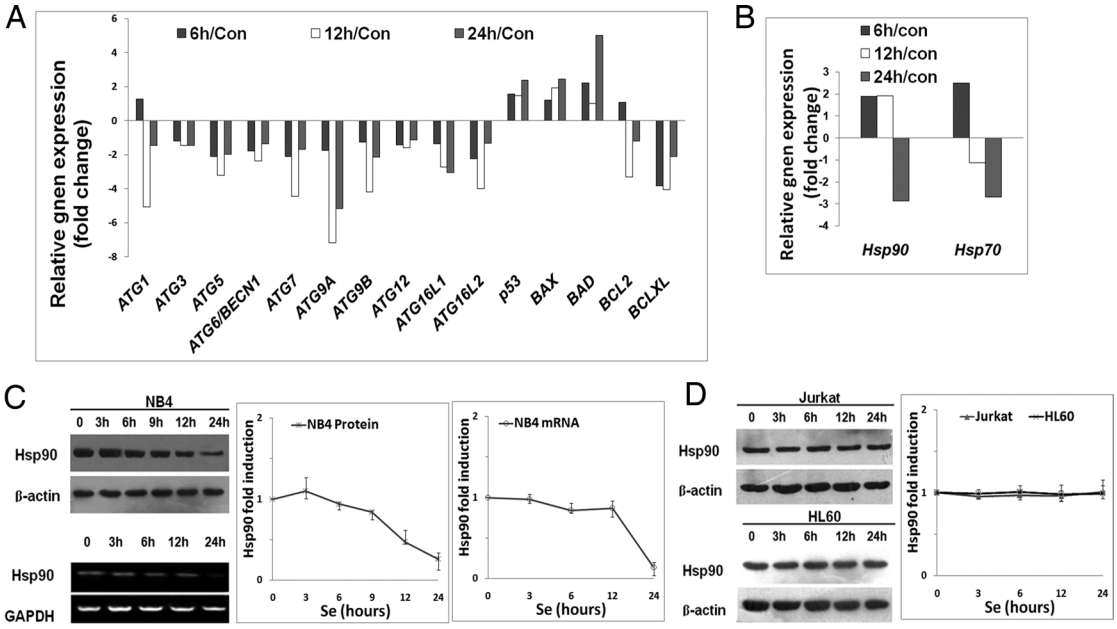

FIGURE 3: Analysis of an RT-PCR autophagy array and detection of Hsp90 expression in different human leukemia cells. (A) The fold change of relative gene expression in sodium selenite–induced NB4 cell apoptotic process at 6, 12, and 24 h from the RT-PCR autophagy array, which included the autophagy-related genes *ATG1, ATG3, ATG5, ATG6/BECN1, ATG7, ATG9A, ATG9B, ATG12, ATG16L,* and *ATG16L2* and the apoptosis-related genes *P53, BAX, BAD, BCL2,* and *BCLXL.* (B) Fold change of the relative gene expression of the chaperone molecules *HSP70* and *HSP90* in selenite-induced NB4 cell apoptosis. (C) Validation of the obtained microarray results by Western blot and standard PCR confirmed Hsp90 down-regulation during selenite treatment in NB4 cells. The left panel shows representative Western blots and PCR results. The middle and right panels show the quantification of normalized Hsp90 levels relative to that of the control. (D) Confirmation of Hsp90 expression by Western blot during selenite treatment in HL60 and Jurkat cells. The left panel shows representative Western blots, and the right panel shows the quantification of normalized Hsp90 levels relative to that of the control. The data are representative of at least three separate experiments.

exposure, but also resulted in down-regulation of LC3 II and the reaccumulation of p62 (Figure 4C). This finding suggests that reducing the expression of Hsp90 was an important step in selenite-induced cell apoptosis and that decreased Hsp90 contributed to autophagy suppression.

The geldanamycin (GA) derivative 17-allylamino-demethoxygeldamycin (17-AAG), which competes with ATP at the ATP binding site and inhibits the intrinsic ATPase activity of Hsp90, is an acknowledged functional inhibitor of Hsp90 (Niikura *et al.*, 2006; Banerji *et al.*, 2008). To better understand the role of Hsp90 in this system, NB4 cells were incubated with 17-AAG. We found that 1 μM 17-AAG could cause apoptosis, and a faster apoptotic rate was detected in the combined treatment group (Figure 4F). However, 17-AAG exposure elevated autophagic levels during apoptosis, which was different from the effect of selenite on autophagy (Figure 4, B and E). Interestingly, the combination of different concentrations of 17-AAG with selenite decreased autophagic levels (Figure 4E). Unfortunately, the explanations for the different effects of selenite and 17-AAG on autophagy were not clear.

Selenite inactivated the IKK/NF-κB signaling pathway in NB4 cells

The results just mentioned demonstrated that Hsp90 down-regulation in the presence of selenite exposure played a critical role in determining the ultimate fate of NB4 cells. We further investigated the mechanism for this process. The IKK/NF-κB pathway was recently reported as the nexus of Hsp90 and autophagy. Therefore we examined the effect of selenite on this pathway in all three cell lines. We found that there was a time-dependent decrease in IKKα, IKKβ, and phospho-NF-κB expression and a remarkable translocation of NF-κB into the cytoplasm from the nucleus in selenite-treated NB4 cells (Figure 5, A and D), suggesting that NF-κB activity was suppressed in the selenite-induced NB4 apoptotic process. Immunofluorescence staining also showed the complete inhibition of the colocalization of NF-κB and 4′,6-diamidino-2-phenylindole (DAPI) in the selenite-treated cells compared with the control group (Figure 5F). The down-regulated expression of IκB was probably due to the decreased activity of its transcription factor, NF-κB (Figure 5A; Wu and Kral, 2005). In contrast, the Western blot results from HL60 and Jurkat cells showed the up-regulation of IKKα, IKKβ, and phospho-NF-κB and the increased nuclear translocation of NF-κB after selenite treatment (Figure 5, B, C, and E), indicating that selenite exhibited different effects on NF-κB activity in different cell lines. The immunostaining in Figure 5F (merged images) confirms that NF-κB localization in the nucleus was induced by selenite in HL60 and Jurkat cells. We demonstrated that the activity of the IKK/NF-κB pathway was suppressed specifically in selenite-induced apoptosis in NB4 cells.

Hsp90 interacted with IKK in all three cell lines

Hsp90 has been reported to interact with IKK in maintaining the latter's activity, thus leading to activation of NF-κB (Qing *et al.*, 2006, 2007). To determine whether Hsp90 mediated the inactivation of the IKK/NF-κB pathway in NB4 cells, a coimmunoprecipitation was performed with an anti-Hsp90 antibody followed by immunoblotting with anti-IKKα or anti-IKKβ antibodies. As shown in Figure 6A, IKKα bound Hsp90 in all three cell lines, but only NB4 cells exhibited decreased expression of IKKα after selenite

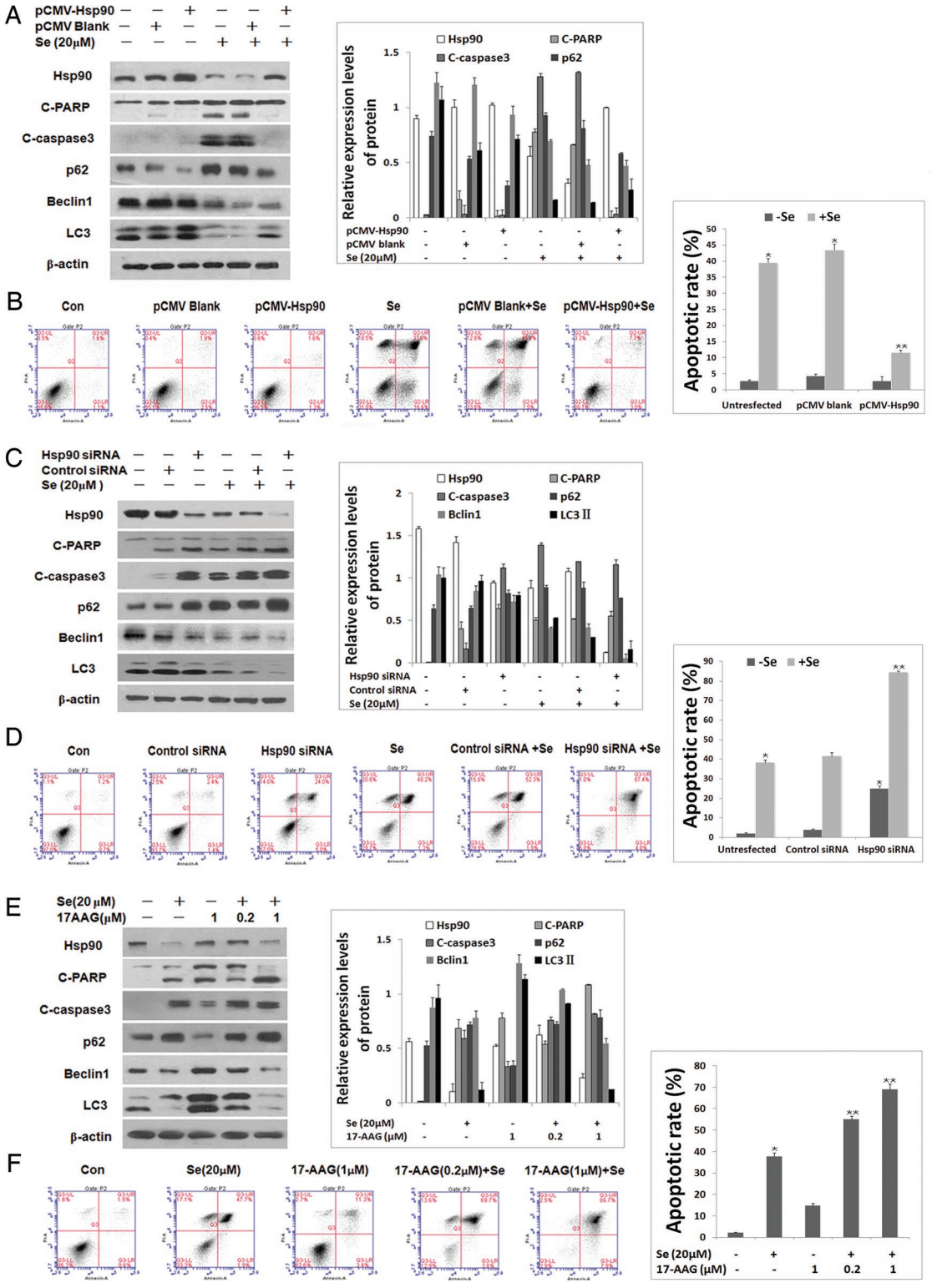

FIGURE 4: Hsp90 is required for selenite-induced apoptosis. (A, C, and E) NB4 cells were transfected with pCMV-Hsp90 and pCMV Blank (negative control) through electroporation (A), transfected with siRNA targeting Hsp90 and nonsilencing scrambled siRNA (C), and incubated with 0.2 or 1 μM 17-AAG for 1.5 h (E). Afterward cells were treated with 20 μM selenite or nothing for 24 h. Cell lysates were analyzed for the levels of Hsp90, cleaved-PARP, cleaved-caspase3, p62, Beclin1, and LC3 via Western blot. The left panels show the representative Western blots, and the right panels show the quantification of normalized protein levels relative to those of the β-actin control. (B, D, and F) The effect of Hsp90 on selenite-induced apoptosis was analyzed by the Annexin-V assay. Following overexpression, insufficient expression, or functional inhibition of Hsp90, NB4 cells were incubated with or without sodium selenite (20 μM) for 24 h and then measured and quantified by flow cytometry as described in *Materials and Methods*. Data are presented as the mean ± SD (n = 3). *$p < 0.01$ compared with control group. **$p < 0.05$ compared with selenite treatment group. The data are representative of at least three separate experiments.

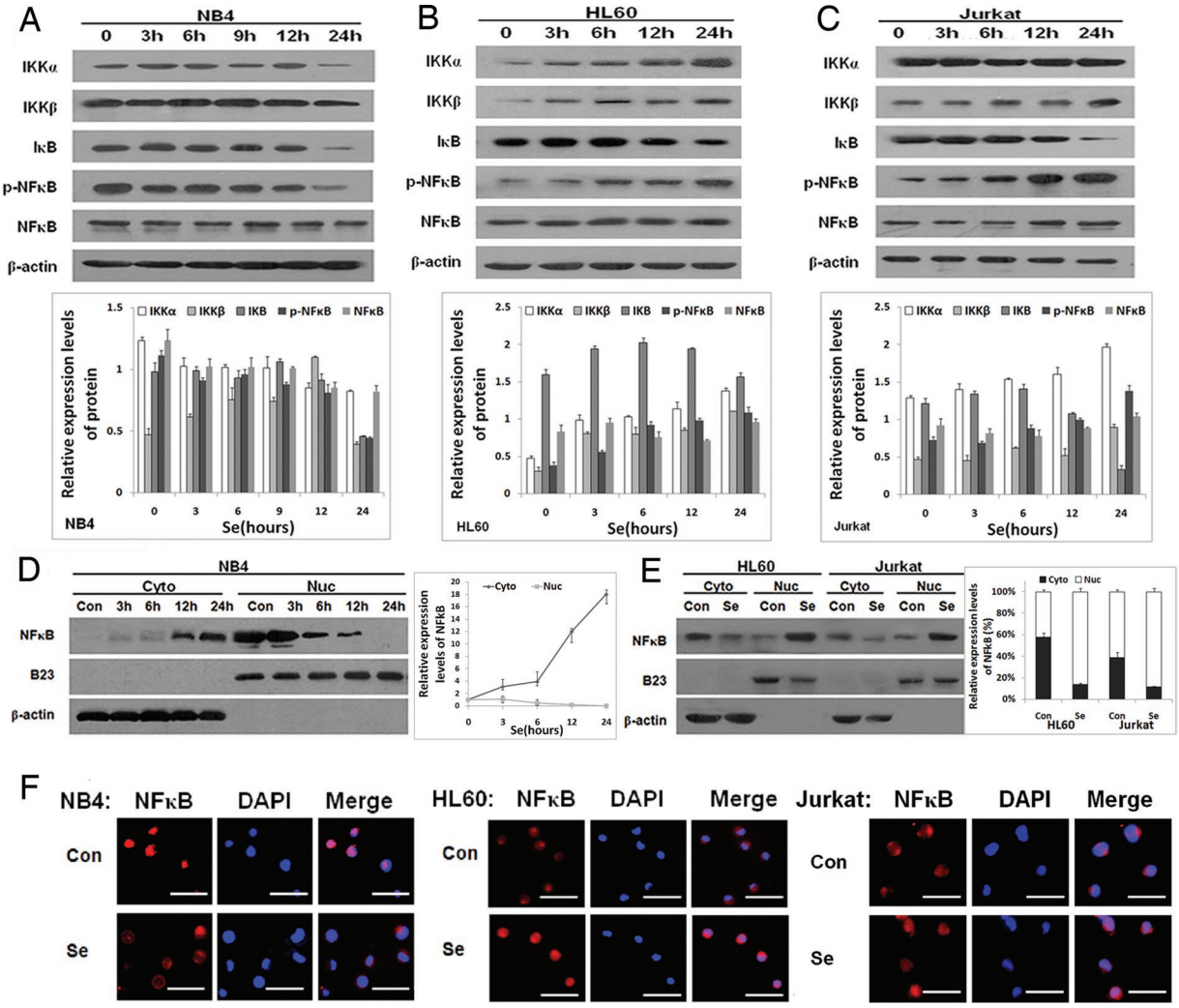

FIGURE 5: Selenite inactivated the IKK/NF-κB signaling pathway in NB4 cells. (A–C) The effect of selenite on the IKK/NF-κB signaling pathway in different cell lines. NB4, HL60, and Jurkat cells were treated with selenite (20 μM) for the indicated times. Then, IKKα, IKKβ, IκB, phospho-NF-κB, and NF-κB were detected by Western blot. The top panels show representative Western blots, and the bottom panels show the quantification of normalized protein levels relative to those of the β-actin control. (D and E) The nucleocytoplasmic translocation of NF-κB induced by selenite in different cell lines. NB4, HL60, and Jurkat cells were exposed to selenite for the indicated times, and the cytoplasmic and nuclear fractions were extracted. NF-κB was detected by Western blot. The purity of cytoplasmic and nuclear proteins was confirmed by β-actin and B23, respectively. The left panels show representative Western blots, and the right panels show the quantification of normalized protein levels relative to those of the β-actin and B23 controls. (F) Immunofluorescence staining results of NF-κB intracellular localization in NB4, HL60, and Jurkat cells treated with or without selenite. The red and blue fluorescence signals represent NF-κB and the nucleus, respectively. The scale bar represents 100 μm. The data are representative of at least three separate experiments.

exposure. Moreover, no interaction was detected between Hsp90 and IKKβ, except in HL60 cells (Figure 6A). Next indirect immunofluorescence experiments were performed to confirm the intracellular localization of Hsp90 and IKKα in NB4 cells. Figure 6B (merged image) shows that the intracellular colocalization of Hsp90 and IKKα was impaired by selenite, indicating a possibility that the proteins may bind to each other in untreated tumor cells. To further elucidate the effect of Hsp90 on NF-κB activity and its subcellular localization, NB4 cells were transfected with pCMV-Hsp90 or Hsp90 targeting siRNA with or without selenite treatment, as described previously. Then the expression of phospho-NF-κB and the localization of NF-κB were examined by Western blot. Figure 6, C and D, shows that the overexpression of Hsp90 restored the selenite-induced decrease of phospho-NF-κB protein levels and facilitated the nuclear localization of NF-κB. Insufficient Hsp90 expression, however, aggravated the phospho-NF-κB reduction and cytoplasmic translocation of NF-κB. The data suggest that the selenite-induced inactivation of NF-κB through the IKK/NF-κB pathway was dependent on Hsp90 expression levels in NB4 cells.

NF-κB is responsible for the transcription of *becn1*

The eukaryotic transcription factor NF-κB was identified as a protein that bound a specific decameric DNA sequence GGG ACT TTC C (Sen and Baltimore, 1986). Recent reports have suggested that there are three NF-κB binding sites (κB sites) in the *becn1* promoter, implying the potential regulatory capacity of NF-κB on autophagy via Beclin1 (Copetti *et al.*, 2009a, 2009b). Treatment with caffeic

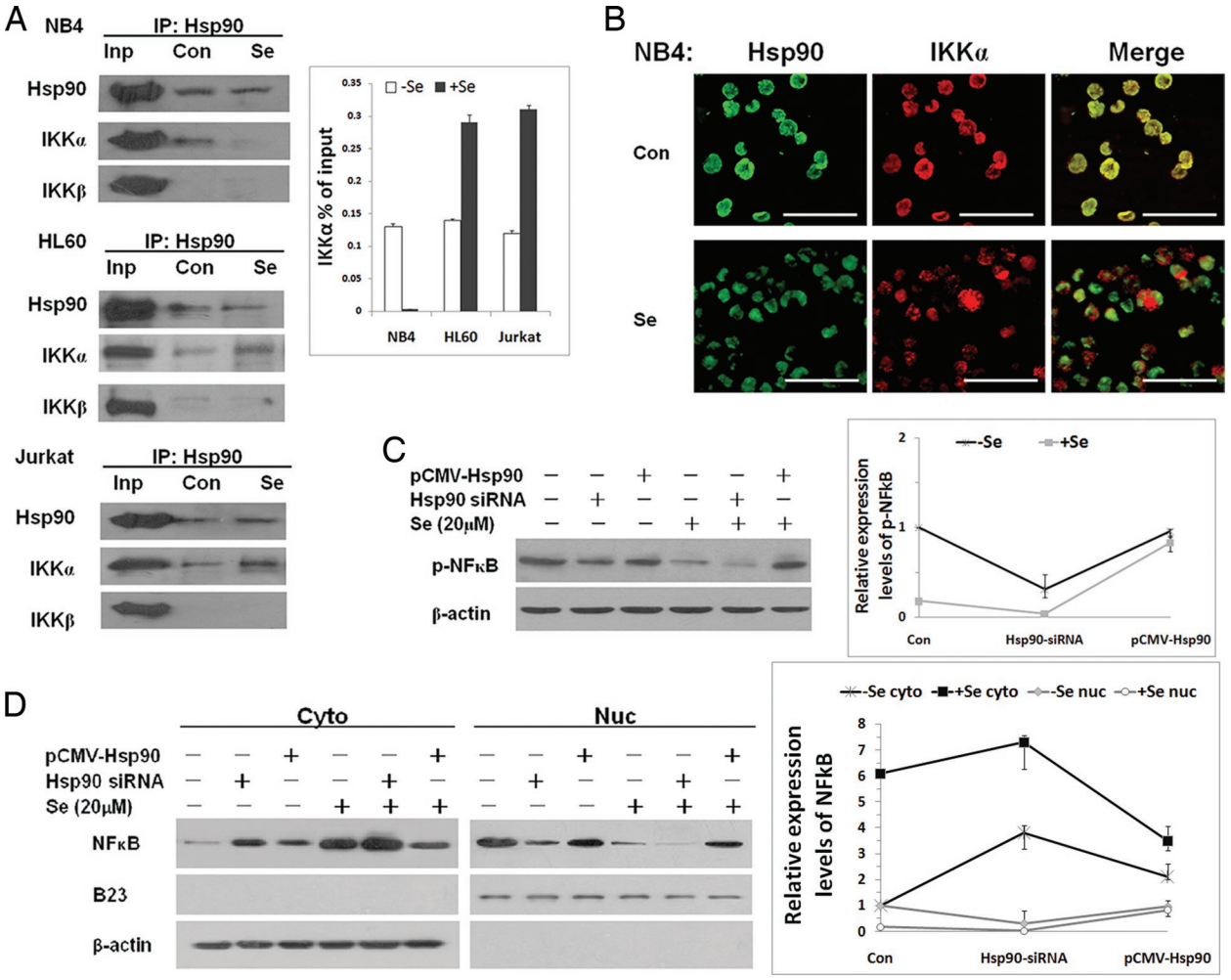

FIGURE 6: Hsp90 interacts with IKK in all three cell lines. (A) The interaction of Hsp90 with IKKα/IKKβ in NB4, HL60, and Jurkat cells as observed by coimmunoprecipitation. Protein extracts prepared from cells were immunoprecipitated with anti-Hsp90 antibodies. The immune complexes and the input (10% of the cell extracts used in the immunoprecipitation step) were analyzed by Western blot with antibodies specific to IKKα or IKKβ. The same membrane was stripped and reprobed to detect Hsp90. The left panel shows representative Western blots, and the right panel shows quantification of normalized protein levels relative to those of the input controls. (B) Indirect immunofluorescence colocalization of Hsp90 and IKKα. NB4 cells were treated with 20 μM selenite for 24 h and analyzed by immunofluorescence microscopy with antibodies to Hsp90 (green) and IKKα (red). The scale bar represents 100 μm. (C and D) The effect of Hsp90 on the activity and cellular localization of NF-κB. NB4 cells were transfected with pCMV-Hsp90 or Hsp90 siRNA by electroporation, as described previously. Then phospho-NF-κB expression from whole cell lysates (C) and NF-κB expression from the cytoplasmic and nuclear fraction (D) were detected by Western blot. The left panels show representative Western blots, and the right panels show the quantification of normalized protein levels relative to those of the β-actin and B23 controls. The data are representative of at least three separate experiments.

acid phenethyl ester (CAPE), a potent inhibitor of NF-κB, led to a substantial decrease in Beclin1 protein in NB4 cells, and the extent of inhibition was increased in the combined selenite treatment group (Figure 7A). Additionally, treatment with 1 μM CAPE alone was sufficient to promote the cleavage of PARP and caspase3 (Figure 7A). The results were verified by Annexin-V/propidium iodide (PI) staining, which showed that the cell apoptotic rate was enhanced by the combined treatment with CAPE compared with the 20 μM selenite treatment alone (Figure 7B). Next we scanned the *becn1* gene for the putative κB sites (GGG ACT TTC C) inside the first intron of the *becn1* promoter (Figure 7C). ChIP was performed to investigate the interaction of NF-κB with the putative κB site in the promoter of *becn1*. Figure 7D shows that, following selenite treatment, the amount of the amplified product in the nontreated group decreased, suggesting that selenite attenuated NF-κB activity and its binding to the *becn1* promoter. Altogether these results demonstrated that NF-κB participated in the autophagy process by regulating Beclin1 expression. To determine whether NF-κB–mediated down-regulation of Beclin1 led to the suppression of autophagy, we examined the effect of selenite on other components of the autophagy core Beclin1–phosphatidylinositol-3-kinase class III (PI3KC3) complex, such as PI3KC3 (a mammalian homologue of yeast Vps34), Ambra-1, and UV irradiation resistance-associated gene (UVRAG). Figure 7E shows that the expression of these proteins decreased in a time-dependent manner, suggesting the gradual disassembly of the complex due to decreased expression of Beclin1. Low concentrations of selenite (2 μM), however, seemed to increase the expression of these proteins (unpublished data). Moreover, like Beclin1, CAPE pretreatment also decreased the expression of PI3KC3, Ambra-1, and UVRAG (Figure 7F).

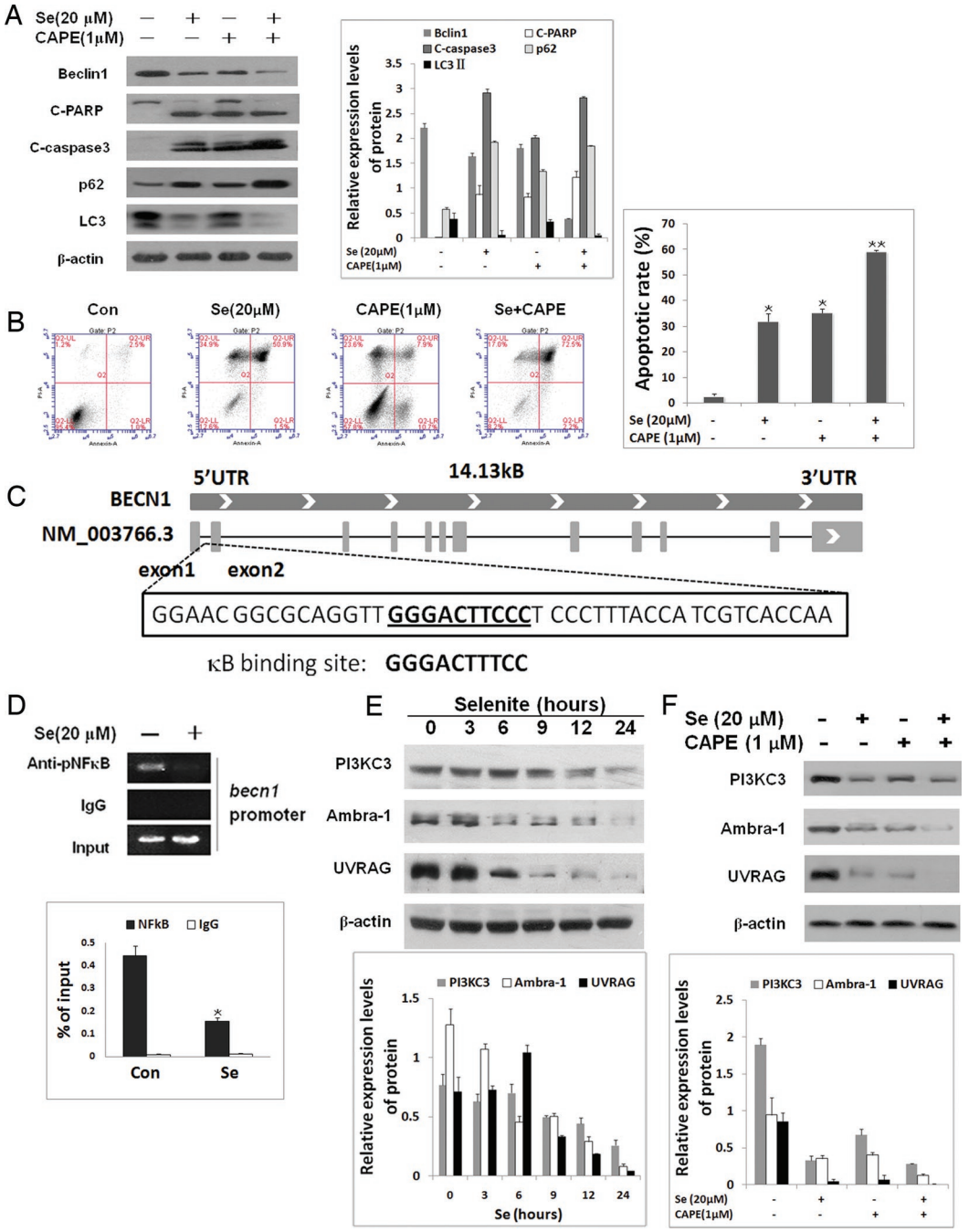

FIGURE 7: NF-κB is responsible for the transcription of *becn1*. (A) The effect of the NF-κB inhibitor CAPE on Beclin1 expression. NB4 cells were incubated with CAPE (1 μM) combined with or without selenite (20 μM) for 24 h. Then, Beclin1, cleaved-PARP, cleaved-caspase3, p62, and LC3 were detected by Western blot. The top panel shows representative Western blots, and the bottom panel shows the quantification of protein levels normalized to those of the β-actin control. (B) NB4 cells treated with 1 μM of the NF-κB inhibitor CAPE and/or selenite were analyzed with an Annexin-V assay. Untreated NB4 cells (Con), selenite-subjected NB4 cells (Se), and inhibitor-treated NB4 cells (CAPE) served as controls. Data are presented as the mean ± SD (n = 3). *$p < 0.01$ compared with control group. **$p < 0.05$ compared with selenite treatment group. (C) The location of primer pairs used for PCR analysis following ChIP. (D) NF-κB ChIP analysis revealed the enrichment of putative NF-κB transcription factor binding sites in *becn1* (κB site) in NB4 cells. The ChIP assay performed with an anti-p-NF-κB antibody was compared with normal rabbit IgG as a negative control. An equal amount (input) of DNA-protein complex was applied (left panel). Real-time PCR quantification of *becn1* promoter sequences in anti-NF-κB ChIP in NB4 cells. Data are expressed as the percentage of input DNA and represent the mean ± SD of triplicate (right panel). (E and F) The effect of selenite or CAPE on the expression of components of the autophagy core complex in NB4 cells. Cells were treated with sodium selenite (20 μM) for different times as indicated (E) and treated with CAPE (1 μM) combined with or without selenite (20 μM) for 24 h (F). Then, PI3KC3, Ambra-1, and UVRAG were detected by Western blot. The top panels show representative Western blots, and the bottom panels show the quantification of normalized protein levels relative to those of the β-actin control. Data are representative of at least three independent experiments.

Altogether these data confirmed that Hsp90-mediated inactivation of NF-κB caused the suppression of autophagy through Beclin1 expression inhibition.

DISCUSSION

Because cancer cells evade programmed cell death to support malignant growth, understanding the mechanisms involved in programmed cell death is critical to developing treatments for various cancers. The work presented here demonstrates a striking difference in the response to sodium selenite between NB4 cell lines and lines derived from other leukemia types with respect to both autophagic levels and NF-κB signaling and provides evidence that Hsp90 is a key regulator responsible for IKK/NF-κB cascade dysfunction in NB4 cells. Hsp90 mediates the eventual transition from autophagic protection to irreversible apoptotic death. These findings also extend our previous observations regarding the importance of Hsp90-mediated autophagy.

Sodium selenite is a common dietary form of selenium, which has chemotherapeutic potential because of its ability to induce cancer cell apoptosis with minimal side effects on normal cells. Our lab has focused on the therapeutic effect of sodium selenite in human leukemia-derived NB4 cells and colorectal cancer–derived SW480 cells. We have shown that augmented reactive oxidant species triggered by sodium selenite can induce NB4 cell apoptosis mainly through the p53-dependent mitochondrial and ER stress–mediated pathways (Li et al., 2003, 2010; Guan *et al.*, 2009). Experiments in vivo have demonstrated the ability of selenite to inhibit colorectal tumor growth in mice without obvious adverse effects on body weight and activities (Huang *et al.*, 2009), providing the possibility of selenite-based therapies for humans in the future. To obtain a more precise mechanistic understanding of the potential role of selenite in cancer therapy, we recently turned our attention to another important cellular process, autophagy, and have detected gradually suppressed autophagy during selenite-induced apoptosis in NB4 cells, indicating that autophagy may antagonize apoptosis by supporting survival in untreated NB4 cells (Ren *et al.*, 2009). Kim *et al.* reported, however, that the generation of superoxide anion triggered by sodium selenite induced mitochondrial damage and subsequent autophagic cell death in malignant glioma cells (Kim *et al.*, 2007), suggesting the concurrence of autophagy and apoptosis in some tumor cells exposed to cytotoxic drugs. Bursch *et al.* also suggested that tamoxifen (TAM) caused dose-dependent autophagy or apoptosis in HL60 cells (Bursch *et al.*, 2008); this finding emphasized the complex interplay between apoptosis and autophagy. Furthermore, autophagic cell death was reported to avoid apoptosis under certain conditions (Hansen *et al.*, 2007). Therefore we examined the effect of selenite on autophagy in two other human leukemia cell lines, HL60 and Jurkat, and they unexpectedly exhibited increased autophagic levels during apoptosis identical to those of glioma cells, but unlike those of NB4 cells. These findings suggested that the effect of selenium on autophagy varied in different cell types, and the actual role of autophagy in cell-fate determination depended on particular circumstances, including the cell types, cell contexts, and properties of the agents.

Hsp90 is a molecular chaperone that contributes to prosurvival signaling in tumor cells. Some studies have characterized Hsp90 as the main chaperone required for the stabilization of multiple oncogenic kinases in the development of acute myelogenous leukemia (Reikvam *et al.*, 2009). Many small molecular chemicals, such as 17-AAG, targeted to Hsp90 inhibition have been used in clinical cancer therapy, suggesting the importance of Hsp90 inhibition in treating the disease (Moser *et al.*, 2009; Taiyab *et al.*, 2009; Wu *et al.*, 2009; Holzbeierlein *et al.*, 2010). Recently we showed that reduced Hsp90 expression was correlated with decreased autophagic levels and higher apoptotic rates in NB4 cells, but not in HL60 and Jurkat cells, indicating a novel function of Hsp90 in signaling switching during selenite treatment.

Having identified that, after selenite exposure, only NB4 cells exhibited reduced Hsp90 expression and that this inhibition was necessary for selenite-triggered apoptosis and autophagy suppression, we aimed to investigate the responsible signaling molecules in this process. Our study identified IKKα as an interacting protein of Hsp90 in all three cell lines, but we examined the dissociation of these proteins in only NB4 cells during selenite-induced apoptosis. IKK is an upstream regulator responsible for the nuclear translocation and activation of NF-κB (Luo *et al.*, 2005). Constitutive activation of the NF-κB pathway is involved in some forms of cancer, such as leukemia, lymphoma, colon cancer, and ovarian cancer (Rayet and Gélinas, 1999). Recently, the direct cross-talk between NF-κB and autophagy was demonstrated. Tumor necrosis factorα–induced NF-κB activation was shown to suppress autophagy, and NF-κB inhibition was found to increase starvation-induced cell death. Autophagy was also described as regulating NF-κB activity (Djavaheri-Mergny *et al.*, 2006, 2007; Djavaheri-Mergny and Codogon, 2007; Nivon *et al.*, 2009). In our experimental settings, endogenous NF-κB was inactivated in NB4 cells after selenite exposure. Overexpression of Hsp90, however, restored the nuclear translocation of NF-κB and partially attenuated selenite-induced cell apoptosis, suggesting that the involvement of Hsp90 down-regulation in selenite-induced cell death occurred mainly through NF-κB activity inhibition. Importantly, the Hsp90–NF-κB link seemed to be present in autophagy as well; thus the cell signaling switch was precisely controlled.

Current knowledge suggests that the Beclin1–Vps34 kinase complex is one of the functional groups in the autophagy machinery, which mediates the localization of other autophagy proteins to the preautophagosomes and is involved in the nucleation of autophagosome formation (Kihara *et al.*, 2001). Beclin1, Vps34, Vps15, and Ambra-1 are considered the common core complex, and UVRAG is usually involved in autophagosome formation and maturation via the regulation of the lipid kinase activity of Vps34 (Itakura *et al.*, 2008). From ChIP assays, we identified *becn1* as the direct target of NF-κB. In addition, the expression levels of other components of the Beclin1/Vps34 core complex were also decreased in conjunction with the down-regulation of Beclin1. Therefore decreased autophagy through Hsp90-mediated NF-κB inactivation was due to the decreased binding of the *becn1* promoter after selenite treatment.

In addition, we found that 17-AAG treatment did not cause decreases in the expression of Hsp90 and Beclin1 (Figure 4E), but it impaired the interaction of Hsp90 with IKK (unpublished data). The different effects of selenite and 17-AAG may be determined by different inhibitory mechanisms. 17-AAG, the inhibitor of Hsp90, has been demonstrated to active a heat shock response and possibly acts through the increased expression of molecular chaperones, in particular through Hsp70 (Niikura *et al.*, 2006; Banerji *et al.*, 2008). Riedel *et al.* reported that 17-AAG induced cytoplasmic alpha-synuclein aggregate clearance by induction of autophagy, suggesting the possible aggregate clearing and autophagy-inducing effects of 17-AAG (Riedel *et al.*, 2010). Selenite, however, functioned in Hsp90-regulated autophagy mainly through decreasing expression of Hsp90. Hence Hsp90 siRNA and 17-AAG exhibited different effects on autophagy. Moreover, our data from two other leukemia cell lines reflected the opposite but supported our views: Following selenite exposure, unchanged Hsp90 expression levels resulted in Hsp90 always binding to the IKK protein such that constitutively

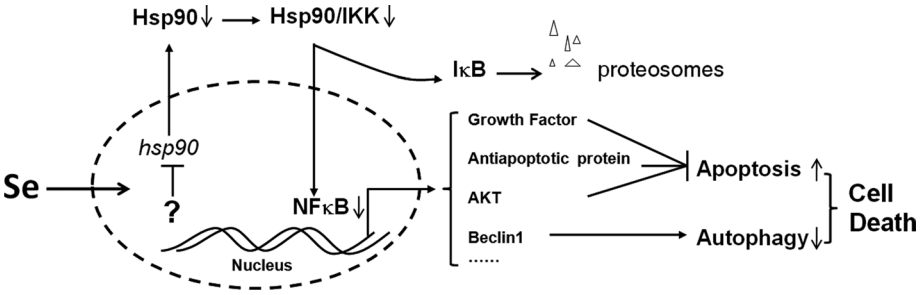

FIGURE 8: The schematic diagram delineating the Hsp90–NF-κB–Beclin1 pathway involved in the selenite-induced apoptosis and autophagy of NB4 cells. Sodium selenite decreased Hsp90 expression, which occurred through some unknown transcription factors and attenuated the interaction of Hsp90 with IKK, which suppressed the activation and nuclear translocation of NF-κB. The inactivated NF-κB then suppressed *becn1* transcription and anti-apoptotic genes, leading to a cell signaling switch from autophagy to apoptosis and, finally, irreversible cell death. This mechanism probably mediates the selenite-induced regulatory balance of apoptosis and autophagy in NB4 cells.

activated NF-κB could translocate into the nucleus and initiate *becn1* transcription. Thus these cells exhibited excessive autophagic levels and led to apoptotic and autophagic cell death.

The tumor suppressor p53 plays a vital role in safeguarding the integrity of the genome. Recently, an emerging area of research has indicated additional activities for p53 in the cytoplasm, where it regulates both apoptosis and autophagy (Levine and Abrams, 2008; Green and Kroemer, 2009; Scherz-Shouval *et al.*, 2010). Our results, schematically summarized in Figure 8, show that Hsp90 was the core regulator in this pathway. The discrepancies in Hsp90 expression among the three selenite-treated leukemia cell lines were possibly due to p53 activity. Recent research revealed that p53 can either inhibit or enhance autophagy and that autophagy can increase or reduce cell survival as a result of certain cellular events and certain signals (Tasdemir *et al.*, 2008a, 2008b). Induction of autophagy by p53 depends on the transactivation of genes such as DRAM (Crighton *et al.*, 2006) and also on the inactivation of the mTOR pathway (Feng *et al.*, 2005). p53 inhibits autophagy through a cytoplasmic (nonnuclear) effect that is correlated with enhanced mTOR activity. Preliminary studies from our laboratory on the p53 status (cloning and sequencing of p53) of our cell lines have suggested that the p53 expressed in the NB4 cell line was wild type (Li *et al.*, 2010) and that the importance of p53 nuclear translocation and activation in selenite-triggered NB4 apoptosis has been elucidated clearly (Guan *et al.*, 2009; Li *et al.*, 2010). Therefore this dual function of p53 indicates a possible mechanism for Hsp90-mediated cell-fate decisions, but the exact mechanism still needs further investigation.

In conclusion, our findings highlight the mechanisms through which Hsp90 regulates the sodium selenite–induced NB4 cell–programmed death process. We show that reduction of Hsp90 in selenite-exposed NB4 cells attenuates the activities of the IKK/NF-κB signaling pathway and leads to the cell signaling switch from autophagy to apoptosis through *becn1* transcriptional inhibition. Importantly, we establish a novel link between apoptosis and autophagy and provide a theoretical basis for the clinical application of sodium selenite in leukemia.

MATERIALS AND METHODS

Cell lines

NB4, HL60, and Jurkat cells were cultured in RPMI 1640 medium with 10% fetal bovine serum, penicillin at 100 U/ml, and streptomycin at 100 μg/ml at 37°C in a 5% CO_2 humidified environment.

Reagents and antibodies

Sodium selenite, 3-MA, bafilomycin A1, rapamycin, CAPE, and anti-β-actin were purchased from Sigma-Aldrich (St. Louis, MO). The chemical inhibitor 17-AAG was purchased from Invitrogen (Carlsbad, CA). GF109203X was purchased from Merck (Darmstadt, Germany). The antibody to Hsp90β used for the Western blot was purchased from Stressgen Biotechnologies (San Diego, CA), and the antibody to Hsp90 for coimmunoprecipitation was purchased from Boster Biological Technology (Wuhan, China). The antibodies for p62 and Ambra-1 were purchased from Abcam (San Francisco, CA). Cleaved caspase-3, cleaved PARP, LC3B, Beclin1, p53, IKKα, IKKβ, IκB, NF-κB, phospho-NF-κB, UVRAG, and PI3KC3 were purchased from Cell Signaling Technology (Danvers, MA). B23 was purchased from Santa Cruz Biotechnology (Santa Cruz, CA).

MDC staining for visualization of autophagic vacuoles

Following treatment with selenite, the autophagic vacuoles were assessed by incubating cells with 50 μM MDC (Sigma) in dimethyl sulfoxide at 37°C for 10 min. After incubation, cells were washed twice with phosphate-buffered saline (PBS) and immediately analyzed and captured by a TE2000-U Nikon Eclipse microscope (Nikon, Tokyo, Japan) operating at 40× magnification. Excitation wavelength = 390 nm; emission wavelength = 460 nm.

PCR array assay

The Human Autophagy RT^2 Profiler PCR Array (SABiosciences, Frederick, MD) was used to study autophagy-specific gene expression profiles in accordance with the manufacturer's recommendations. Briefly, total RNA was isolated from different experimental groups using Trizol (Invitrogen). Potential genomic DNA contamination was removed from the samples by treatment with RNase-free DNase (Invitrogen) for 15 min at 37°C. The RNA concentration and purity were determined with a NanoDrop ND-1000 (Thermo Scientific). RNA quality was evaluated by electrophoresis. The first strand cDNA was synthesized from 1–2 μg of total RNA using SuperScript III Reverse Transcriptase (Invitrogen). After synthesis, real-time PCR was performed with the SuperArray PCR master mix and iCycler iQ5 multi-color detection system (Bio-Rad Laboratories, Hercules, CA) according to the manufacturer's instructions. The amplification data (fold changes in C_t values of all the genes) were analyzed by the $\Delta\Delta C_t$ method.

Flow cytometric analysis for apoptosis

The detection was performed according to the manual included with the Annexin V–fluorescein isothiocyanate (FITC) apoptosis detection kit (Calbiochem, San Diego, CA). Approximately 10^6 cells were harvested, washed twice with ice-cold PBS, and stained with 0.5 ml of binding buffer containing 1.25 μl of Annexin V-FITC. After incubation in the dark for 15 min at room temperature, the cells were collected and resuspended in the binding buffer containing PI. Flow cytometry was performed on an Accuri (Ann Arbor, MI) C6 Flow Cytometer to detect apoptosis.

Western blot analysis

Cells were lysed in RIPA buffer (20 mM Tris, pH 7.5; 150 mM NaCl; 1 mM EDTA; 1 mM EGTA; 1% Triton X-100; 2.5 mM sodium pyrophosphate; 1 mM β-glycerophosphate; 1 mM Na_3VO_4; leupeptin at 1 μg/ml, 1 mM phenylmethylsulfonyl fluoride [PMSF]) and subjected to sonication for 30 s. The cell lysates were centrifuged at 12,000 × *g* for 15 min at 4°C, and the supernatant was collected. The protein concentrations were determined by the Bradford assay. After normalization, equal amounts of proteins were fractionated onto 8–15% SDS–PAGE gels and then transferred to nitrocellulose membranes. The membranes were blocked with 5% nonfat milk in Tris-buffered saline–Tween-20 and probed with primary antibodies followed by horseradish peroxidase–labeled secondary antibodies; the blots were probed with the SuperSignal West Pico Chemiluminescent Substrate (Thermo Scientific) system to visualize the immunoreactive bands.

RT-PCR

Total RNA was extracted with Trizol (Invitrogen), according to the manufacturer's instructions. RT was carried out with 500 ng total RNA from cells using M-MLV, and the resultant cDNA was subjected to PCR. Primers for *HSP90* (forward 5′-CCT TCT ATT TGT CCC ACG -3′; reverse 5′-ATC CTC CGA GTC TAC CAC -3′) were synthesized and purchased from Sangon Biotech (Shanghai Co., China).

Extraction of cytoplasmic and nuclear fractions

Harvested cells were washed twice with ice-cold PBS and rapidly resuspended in cytoplasmic extraction reagent (Boster Biological Technology) on ice for 30 min. Then the cells were pelleted at 12,000 × *g* for 10 min at 4°C, and the supernatant was collected as the cytoplasmic fraction. The nuclear pellet was resuspended in 50 μl nuclear extraction reagent (Boster Biological Technology), and the mixture was incubated on ice for 30 min, vortexed 6× 10 s, and centrifuged at 12,000 × *g* for 10 min at 4°C. The supernatant was collected as the nuclear fraction. PMSF and leupeptin were added into both the cytoplasmic and the nuclear extraction reagents before use.

Coimmunoprecipitation

Cells were harvested and lysed using RIPA. The protein concentrations were measured using the Bradford method. Aliquots (200 μg) of cellular proteins were precleared by adding 2 μl of the appropriate normal immunoglobulin G (IgG) to 25 μl of appropriate protein A+G-agarose conjugate (Santa Cruz) overnight at 4°C. The immunoprecipitation was performed with the appropriate antibody for 3 h at 4°C. Complexes bound to the protein A+G-agarose conjugate were washed four times with RIPA and separated by SDS–PAGE. Western blot analysis was performed as previously described.

Electroporation

The eukaryotic expression vector pCMV-Hsp90 was a gift from Y.F. Shen (Peking Union Medical College, Beijing, China). The Hsp90-specific siRNA (sense 5′-GAU CAG ACA GAG UAC CUA G-3′; antisense 5′-CUA GGU ACU CUG UCU GAU C-3′) and nonsilencing scrambled siRNA were synthesized and purchased from GenePharma (Shanghai, China). The collected cells were washed twice with serum and antibiotic-free RPMI 1640 medium and resuspended to achieve a final concentration of 1.3×10^7 cells/ml. Subsequently, 430 μl of the cell suspension was mixed with 10 μg of plasmid DNA or siRNA and electroporated in a 0.4-cm cuvette using the MicroPulser electroporation apparatus (Bio-Rad Laboratories) following a single-pulse protocol (voltage, 250 V; capacitance, 950 μF). Under these conditions, we consistently reached a transfection efficiency of 60% or more (verified by Western blot) without significant reductions in viability. Sixteen hours after transfection, cells were treated with different compounds and harvested at a given time for subsequent research.

Immunofluorescence

Cells were grown and treated for the indicated number of hours. After they were washed three times with ice-cold PBS, the cells were fixed with methanol for 10 min, washed three times with PBS, and blocked with 1% Triton X-100 in PBS for 30 min at room temperature. Then, the cells were incubated with the appropriate antibody diluted 1:100 (vol/vol) in PBS overnight at 4°C, followed by FITC- or CY3-conjugated secondary antibodies (Jackson ImmunoResearch Laboratories, West Grove, PA) diluted 1:150 (vol/vol) in PBS at room temperature for 1 h. After the cells were washed with PBS, they were stained with 1 μM DAPI (Sigma-Aldrich) for 5 min. Images were captured with a TE2000-U Nikon Eclipse microscope.

ChIP assay

The target chromatin was extracted and immunoprecipitated with a SimpleChIP Enzymatic Chromatin IP Kit (Cell Signaling Technology) according to the manufacturer's instructions. Protein complexes were cross-linked to DNA in living nuclei by adding formaldehyde (Sigma) directly to the tissue culture medium to a final concentration of 1%. Cross-linking was allowed to proceed for 10 min at room temperature and was then stopped by the addition of glycine to a final concentration of 0.125 M. The cross-linked cells were washed with PBS and swelled in Buffer A on ice for 10 min. The nuclei were pelleted by centrifugation at 3000 rpm for 5 min at 4°C and lysed by incubation in Buffer B with 0.5 mM dithiothreitol. The resulting chromatin solution was digested with micrococcal nuclease for 20 min at 37°C to generate 150–900 base pair DNA fragments. After the digestion was stopped with 0.5 M EDTA, the nuclei were pelleted by centrifugation at 13,000 rpm for 1 min at 4°C and resuspended in ChIP Buffer on ice for 10 min. The lysates were sonicated with five pulses of 10 s at 30% power to break the nuclear membranes. After microcentrifugation, the supernatant was divided into aliquots. Then, 2 μg of anti-phospho-NF-κB was added to each aliquot of chromatin and incubated for 12–16 h at 4°C with rotation. Antibody-protein-DNA complexes were isolated by immunoprecipitation with ChIP-Grade Protein G Agarose Beads for 2 h at 4°C with rotation. Following extensive washing, bound DNA fragments were eluted and analyzed by subsequent standard PCR and real-time PCR using primers specific for the *becn1* promoters. The primers for the κB site in the *becn1* promoter (forward 5′- CCC GTA TCA TAC CAT TCC TAG-3′; reverse 5′- GAA ACT CGT GTC CAG TTT CAG-3′) were synthesized and purchased from Sangon Biotech (Shanghai, China).

Statistical analysis

All experiments were repeated at least three times. The results are expressed as the mean ± SD ($n \geq 3$). In some cases, Student's *t* test was used for comparing two groups. A statistically significant difference was set at $p < 0.05$.

ACKNOWLEDGMENTS

We thank Y.F. Shen for providing the Hsp90 plasmid as detailed in the text. This work was supported by grants from the National Natural Sciences Foundation of China (No. 30770491 and No. 30970655), the Beijing Natural Science Foundation (No. 5082015), the National

Laboratory of Medical Molecular Biology Special Fund (No. 2060204), and the Ministry of Education, China, for Doctor-training Unite (No. 20091106110025).

REFERENCES

Asfour IA, Shazly SE, Fayek MH, Hegab HM, Raouf S, Moussa MA (2006). Effect of high-dose sodium selenite therapy on polymorphonuclear leukocyte apoptosis in nonHodgkin's lymphoma patients. Biol Trace Elem Res 110, 19–32.

Banerji U *et al*. (2008). An in vitro and in vivo study of the combination of the heat shock protein inhibitor 17-allylamino-17-demethoxygeldanamycin and carboplatin in human ovarian cancer models. Cancer Chemother Pharmacol 62, 769–778.

Biederbick A, Kern HF, Elsasser HP (1995). Monodansylcadaverine (MDC) is a specific in vivo marker for autophagic vacuoles. Eur J Cell Biol 66, 3–14.

Bursch W *et al*. (2008). Cell death and autophagy: cytokines, drugs, and nutritional factors. Toxicology 254, 147–157.

Crighton D, Wilkinson S, O'Prey J, Syed N, Smith P, Harrison PR, Gasco M, Garrone O, Crook T, Ryan KM (2006). DRAM, a p53-induced modulator of autophagy, is critical for apoptosis. Cell 126, 121–134.

Copetti T, Bertoli C, Dalla E, Demarchi F, Schneider C (2009a). p65/RelA modulates BECN1 transcription and autophagy. Mol Cell Biol 29, 2594–2608.

Copetti T, Demarchi F, Schneider C (2009b). p65/RelA binds and activates the beclin 1 promoter. Autophagy 5, 858–859.

Cullinan SB, Whitesell L (2006). Heat shock protein 90: A unique chemotherapeutic target. Semin Oncol 33, 457–465.

Daniel JK, Scott DE (2000). Autophagy as a regulated pathway of cellular degradation. Science 290, 1717–1721.

Djavaheri-Mergny M, Amelotti M, Mathieu J, Beasncon F, Bauvy C, Codogno P (2007). Regulation of autophagy by NFκB transcription factor and reactive oxygen species. Autophagy 3, 390–392.

Djavaheri-Mergny M, Amelotti M, Mathieu J, Besancon F, Bauvy C, Souquère S, Pierron G, Codogno P (2006). NF-kappaB activation represses tumor necrosis factor-alpha-induced autophagy. J Biol Chem 281, 30373–30382.

Djavaheri-Mergny M, Codogon P (2007). Autophagy joins the game to regulate NF-kappaB signaling pathways. Cell Res 17, 576–577.

Feng Z, Zhang H, Levine AJ, Jin S (2005). The coordinate regulation of the p53 and mTOR pathways in cells. Proc Natl Acad Sci USA 102, 8204–8209.

Green DR, Kroemer G (2009). Cytoplasmic functions of the tumour suppressor p53. Nature 458, 1127–1130.

Guan L, Han B, Li Z, Hua F, Huang F, Wei W, Yang Y, Xu C (2009). Sodium selenite induces apoptosis by ROS-mediated endoplasmic reticulum stress and mitochondrial dysfunction in human acute promyelocytic leukemia NB4 cells. Apoptosis 14, 218–225.

Habib GM (2009). p53 regulates Hsp90beta during arsenite-induced cytotoxicity in glutathione-deficient cells. Arch Biochem Biophys 481, 101–109.

Hansen K, Wagner B, Hamel W, Schweizer M, Haag F, Westphal M, Lamszus K (2007). Autophagic cell death induced by TrkA receptor activation in human glioblastoma cells. J Neurochem 103, 259–275.

Holzbeierlein JM, Windsperger A, Vielhauer G (2010). Hsp90: a drug target? Curr Oncol Rep 12, 95–101.

Huang F, Nie C, Yang Y, Yue W, Ren Y, Shang Y, Wang X, Jin H, Xu C, Chen Q (2009). Selenite induces redox-dependent Bax activation and apoptosis in colorectal cancer cells. Free Radic Biol Med 46, 1186–1196.

Itakura E, Kishi C, Inoue K, Mizushima N (2008). Beclin 1 forms two distinct phosphatidylinositol 3-kinase complexes with mammalian Atg14 and UVRAG. Mol Biol Cell 19, 5360–5372.

Iwai-Kanai E, Yuan H, Huang C, Sayen MR, Perry-Garza CN, Kim L, Gottlieb RA (2008). A method to measure cardiac autophagic flux in vivo. Autophagy 4, 322–329.

Jiang H, Cheng D, Liu W, Peng J, Feng J (2010). Protein kinase C inhibits autophagy and phosphorylates LC3. Biochem Biophys Res Commun 395, 471–476.

Karantza-Wadsworth V, White E (2007). Role of autophagy in breast cancer. Autophagy 3, 610–613.

Kihara A, Kabeya Y, Ohsumi Y, Yoshimori T (2001). Beclin-phosphatidylinositol 3-kinase complex functions at the trans-Golgi network. EMBO Rep 2, 330–335.

Kim EH, Sohn S, Kwon HJ, Kim SU, Kim MJ, Lee SJ, Choi KS (2007). Sodium selenite induces superoxide-mediated mitochondrial damage and subsequent autophagic cell death in malignant glioma cells. Cancer Res 67, 6314–6324.

Levine B, Abrams J (2008). p53: The Janus of autophagy? Nat Cell Biol 10, 637–639.

Levine B, Yuan J (2005). Autophagy in cell death: an innocent convict? J Clin Invest 115, 2679–2688.

Li J, Zuo L, Shen T, Xu CM, Zhang ZN (2003). Induction of apoptosis by sodium selenite in human acute promyelocytic leukemia NB4 cells: involvement of oxidative stress and mitochondria. J Trace Elem Med Biol 17, 19–26.

Li Z, Shi K, Guan L, Cao T, Jiang Q, Yang Y, Xu C (2010). ROS leads to MnSOD upregulation through ERK2 translocation and p53 activation in selenite-induced apoptosis of NB4 cells. FEBS lett 584, 2291–2297.

Luo JL, Kamata H, Karin M (2005). IKK/NF-κB signaling: balancing life and death - a new approach to cancer therapy. J Clin Invest 115, 2625–2632.

Mahalingam D, Swords R, Carew JS, Nawrocki ST, Bhalla K, Giles FJ (2009). Targeting HSP90 for cancer therapy. Br J Cancer 100, 1523–1529.

Maiuri MC, Zalckvar E, Kimchi A, Kroemer G (2007). Self-eating and self-killing: crosstalk between autophagy and apoptosis. Nat Rev Mol Cell Biol 8, 741–752.

Moser C, Lang SA, Stoeltzing O (2009). Heat-shock protein 90 (Hsp90) as a molecular target for therapy of gastrointestinal cancer. Anticancer Res 29, 2031–2042.

Neckers L, Ivy SP (2003). Heat shock protein 90. Curr Opin Oncol 15, 419–424.

Niikura Y, Ohta S, Vandenbeldt KJ, Abdulle R, McEwen BF, Kitagawa K (2006). 17-AAG, an Hsp90 inhibitor, causes kinetochore defects: a novel mechanism by which 17-AAG inhibits cell proliferation. Oncogene 25, 4133–4146.

Nivon M, Richet E, Codogno P, Arrigo AP, Kretz-Remy C (2009). Autophagy activation by NFkappaB is essential for cell survival after heat shock. Autophagy 5, 766–783.

Pattingre S, Tassa A, Qu X, Garuti R, Liang XH, Mizushima N, Packer M, Schneider MD, Levine B (2005). Bcl-2 antiapoptotic proteins inhibit Beclin 1-dependent autophagy. Cell 122, 927–939.

Portugal J, Bataller M, Mansilla S (2009). Cell death pathways in response to antitumor therapy. Tumori 95, 409–421.

Qing G, Yan P, Qu Z, Liu H, Xiao G (2007). Hsp90 regulates processing of NF-κB2 p100 involving protection of NF-κB-inducing kinase (NIK) from autophagy-mediated degradation. Cell Res 17, 520–530.

Qing G, Yan P, Xiao G (2006). Hsp90 inhibition results in autophagy-mediated proteasome-independent degradation of IκB kinase (IKK). Cell Res 16, 895–901.

Rayet B, Gélinas C (1999). Aberrant rel/nfkb genes and activity in human cancer. Oncogene 18, 6938–6947.

Reikvam H, Ersvaer E, Bruserud O (2009). Heat shock protein 90—a potential target in the treatment of human acute myelogenous leukemia. Curr Cancer Drug Targets 9, 761–776.

Ren Y, Huang F, Liu Y, Yang Y, Jiang Q, Xu C (2009). Autophagy inhibition through PI3K/Akt increases apoptosis by sodium selenite in NB4 cells. BMB Rep 42, 599–604.

Riedel M, Goldbaum O, Schwarz L, Schmitt S, Richter-Landsberg C (2010). 17-AAG induces cytoplasmic alpha-synuclein aggregate clearance by induction of autophagy. PLoS One 5, e8753.

Sanmartin C, Plano D, Palop JA (2008). Selenium compounds and apoptotic modulation: a new perspective in cancer therapy. Mini Rev Med Chem 8, 1020–1031.

Scherz-Shouval R, Weidberg H, Gonen C, Wilder S, Elazar Z, Oren M (2010). p53-dependent regulation of autophagy protein LC3 supports cancer cell survival under prolonged starvation. Proc Natl Acad Sci USA Epub ahead of print.

Sen R, Baltimore D (1986). Multiple nuclear factors interact with the immunoglobulin enhancer sequences. Cell 46, 705–716.

Sinha R, El-Bayoumy K (2004). Apoptosis is a critical cellular event in cancer chemoprevention and chemotherapy by selenium compounds. Curr Cancer Drug Targets 4, 13–28.

Taiyab A, Sreedhar AS, Rao ChM (2009). Hsp90 inhibitors, GA and 17AAG, lead to ER stress-induced apoptosis in rat histiocytoma. Biochem Pharmacol 78, 142–152.

Tasdemir E *et al*. (2008a). Regulation of autophagy by cytoplasmic p53. Nat Cell Biol 10, 676–687.

Tasdemir E, Chiara Maiuri M, Morselli E, Criollo A, D'Amelio M, Djavaheri-Mergny M, Cecconi F, Tavernarakis N, Kroemer G (2008b). A dual role of p53 in the control of autophagy. Autophagy 4, 810–814.

Tsujimoto Y, Shimizu S (2005). Another way to die: autophagic programmed cell death. Cell Death Differ 12, Suppl 21528–1534.
Wu JT, Kral JG (2005). The NF-kappaB/IkappaB signaling system: a molecular target in breast cancer therapy. J Surg Res 123, 158–169.
Wu YC, Yen WY, Lee TC, Yih LH (2009). Heat shock protein inhibitors, 17-DMAG and KNK437, enhance arsenic trioxide-induced mitotic apoptosis. Toxicol Appl Pharmacol 236, 231–238.
Xiao G (2007). Autophagy and NF-κB: Fight for fate. Cytokine Growth Factor Rev 18, 233–243.
Zhang Y, Wang JS, Chen LL, Zhang Y, Cheng XK, Heng FY, Wu NH, Shen YF (2004). Repression of hsp90beta gene by p53 in UV irradiation-induced apoptosis of Jurkat cells. J Biol Chem 279, 42545–42551.
Zuehlke A, Johnson JL (2010). Hsp90 and cochaperones twist the functions of diverse client proteins. Biopolymers 93, 211–217.